

Received September 18, 2021, accepted October 2, 2021, date of publication October 4, 2021, date of current version October 19, 2021.

Digital Object Identifier 10.1109/ACCESS.2021.3117947

High Misalignment Tolerance in Efficiency of WPT System With Movable Intermediate Coil and Adjustable Frequency

LIBO TIAN¹, FUYAO YANG², BO CAI², SONG LI³, KUN LIU³,
AND HAISEN ZHAO^{1,3}, (Senior Member, IEEE)

¹School of Mechanical and Electrical Engineering, Shijiazhuang University, Shijiazhuang 050035, China

²State Key Laboratory of Advanced Power Transmission Technology, Global Energy Interconnection Research Institute Company, Ltd., Beijing 102211, China

³State Key Laboratory of Alternate Electrical Power System With Renewable Energy Sources, North China Electric Power University (NCEPU), Beijing 102206, China

Corresponding author: Haisen Zhao (zhaohaisen@163.com)

This work was supported in part by the Science and Technology Project of State Grid Corporation of China under Grant 7000-201958480A-0-00, and in part by the Shijiazhuang Science and Technology Research and Development Plan Project under Grant 201060871.

ABSTRACT Offsets between the primary and secondary coils of loosely coupled transformers (LCT) are attributable to the efficiency decline of the wireless power transfer (WPT) system. To improve the misalignment tolerance of efficiency in WPT system, this paper presents a LCT system with a movable intermediate coil and adjustable system frequency, which can promote the efficiency of the WPT system under misalignment condition. First, the influences of the position and compensation parameter of intermediate coil on the system efficiency during migration are summarized. The optimal compensation parameter and optimal position selection method of intermediate coil are proposed. Then, the influence of frequency on system efficiency is studied, and the detailed control strategy of intermediate coil's position and system frequency is proposed. A 3-kW prototype WPT with the proposed three-coil LCT is manufactured and experimental validations are also performed. The results show that the efficiency declines of three-coil LCT with the proposed control strategy is 1.8% when the lateral offsets reach 300mm, namely 43% of the outer diameter of coil.

INDEX TERMS Wireless power transfer (WPT), loosely coupled transformer (LCT), adjustable system frequency, movable intermediate coil, misalignment tolerance of efficiency.


I. INTRODUCTION

Owing to the rapid growth of the electric vehicle (EV) industry, obvious momentum in research of energy storage system charging was witnessed in the last few years [1]. Among the feasible charging solutions are the wireless power transfer (WPT) systems [2]–[4]. Although the performance of these WPTs can meet the efficiency requirements at certain occasions, the efficiencies of the WPT system witness an obvious decline when the primary and secondary coils are misaligned.

The suppression of system efficiency decline is equivalent to the strength of the misalignment tolerance of efficiency under offset conditions. Various approaches were proposed for achieving higher misalignment tolerance of the WPT

efficiency [5], [7], [8]. These methods can be divided into the following categories: 1) loosely coupled transformer (LCT) design; 2) compensation topology design; and 3) control methods.

As for the optimal design of LCT, a double D-shaped (DD) coil and a DD-quadrature (DDQ) coil with additional orthogonal coil were proposed on the primary side [9] and the EV side [10], respectively, for improving the misalignment tolerance of WPT's efficiency. However, considering that the DDQ coil increases the use of wires, the bipolar pad (BP) coil partially overlapping DD coils was proposed in [11]. In addition, it is revealed that the square coil is more suitable for WPT application [12]. In [13], a flux pipe coupler was designed which has a significantly improved flux path. In [14], Quad-D-quadrature (QDQ) was proposed to improve the misalignment performance.

The associate editor coordinating the review of this manuscript and approving it for publication was Lin Zhang .

The number of turns and the quality factors of coils were also optimized [13]. It was also verified that I/N-type core can improve the lateral misalignment tolerance of the dynamic WPT's efficiency [14]. Moreover, to further improve the system's efficiency, several methods were proposed, such as the nonlinear thickness ferrite core [15], field-type ferrite core [2], non-linear ferrite core [16], EE/CC-type ferrite core [17], multi-coil LCT [5], [18], [19], etc.

Furthermore, a compensation topology named L/C was adopted to improve the efficiency of WPT [20]. Reviewing six types of compensation topologies, the series-series (SS) and series-parallel (SP) compensation circuits were presented for efficiency improvement in [21]. However, the double-sided inductor-capacitor-capacitor compensation, which is LCC topology, is less sensitive to mistuning than other topologies [22]. Therefore, it can be used to improve the misalignment tolerance of WPT's efficiency. To obtain the higher misalignment tolerance of efficiency, a variable inductor (VI) was inserted in the primary circuit for compensating the additional reactance [23]. However, the volume of WPT was increased. Moreover, a design considering compensation capacitor was proposed in [24], and the lateral misalignment tolerance was extended to 44.3% of the coupler's size. The above measures can improve the misalignment tolerance of efficiency to some extent, but they adopted a more complex structure, compensating topology, and even complex control strategy.

A third coil is used to reversely connect with the primary coil in [25], improving the misalignment tolerance in both x- and y- directions. The application of passive intermediate coil in WPT system is also widely studied. In [26], a WPT system with an intermediate coil is analyzed, and an optimal design method is proposed for high system efficiency. Therefore, three-coil system with an additional coil can improve the misalignment tolerance of efficiency. In the application of electric vehicle wireless charging, the primary coil is fixed on the ground and the secondary coil is installed on vehicle. When the secondary coil is not aligned, only the intermediate coil without power cable can be move freely. In addition, compared with two-coil system, the intermediate coil can get rid of the restriction of the power cable. However, when the secondary coil is not aligned with the primary coil, the influence of a movable intermediate coil on the misalignment tolerance has not been studied.

To improve the misalignment tolerance of the WPT's efficiency with a simple structure or simple control strategy, a novel LCT with intermediate coil and control strategy of intermediate coil's position and system frequency is proposed. First, the characteristics of the intermediate coil's compensation parameter are analyzed. Furthermore, the influences of the intermediate coil's position and system frequency on the system efficiency during migration are studied, and a detailed control strategy of the intermediate coil's position and system frequency is proposed. Finally, the effect to promote misalignment tolerance of the proposed control strategy in this paper is verified on a 3-kW LCT.

II. EQUIVALENT CIRCUIT OF TWO-COIL AND THREE-COIL LCT

A. EQUIVALENT CIRCUIT MODELING OF TWO-COIL LCT

The equivalent circuit model of the two-coil LCT with series-series (SS) compensation is shown in Fig.1, where U_p is the high-frequency supply; L_p and L_s are the self-inductances of the primary and secondary coils, respectively; R_p and R_s are the resistances of the coils, respectively; C_p and C_s are the compensation capacitance of the coils; respectively, M_{ps} is the mutual inductance between the primary and secondary coils, and R_{eq} is the equivalent resistance of the load.

According to the equivalent circuit and *Kirchhoff's law*, the equations of the output power and efficiency of the resonant two-coil LCT are represented in (1) and (2).

$$P_{out} = \frac{U_p^2 \omega^2 M_{ps}^2 R_{eq}}{\left[R_p (R_s + R_{eq}) + \omega^2 M_{ps}^2 \right]^2} \quad (1)$$

$$\eta = \frac{\omega^2 M_{ps}^2 R_{eq}}{\left[R_p (R_s + R_{eq}) + \omega^2 M_{ps}^2 \right] (R_s + R_{eq})} \quad (2)$$

B. EQUIVALENT CIRCUIT MODELING OF THREE-COIL LCT

The equivalent circuit model of the three-coil LCT is shown in Fig.2, where L_i is the self-inductance of intermediate coil, C_i and R_i stand for the compensation capacitance and resistance of the intermediate coil, respectively. Similarly, the following equations can be deduced.

$$\dot{U}_p = Z_p \dot{I}_p - j\omega M_{pi} \dot{I}_i - j\omega M_{ps} \dot{I}_s \quad (3)$$

$$0 = -j\omega M_{pi} \dot{I}_p + Z_i \dot{I}_i + j\omega M_{is} \dot{I}_s \quad (4)$$

$$0 = -j\omega M_{ps} \dot{I}_p + j\omega M_{is} \dot{I}_i + Z_s \dot{I}_s \quad (5)$$

where Z_p , Z_s and Z_i are the equivalent impedance of the primary, secondary and intermediate circuit loop, respectively, and can be expressed by (6), (7) and (8), respectively.

$$Z_p = R_p + j\omega L_p + \frac{1}{j\omega C_p} \quad (6)$$

$$Z_s = R_s + R_{eq} + j\omega L_s + \frac{1}{j\omega C_s} \quad (7)$$

$$Z_i = R_i + j\omega L_i + \frac{1}{j\omega C_i} \quad (8)$$

Substituting (6), (7) and (8) into (3), (4) and (5), respectively, and the current in each circuit loop can be deduced as follows, (9)–(11), as shown at the bottom of the next page.

According to (9), (10), and (11), output power and the efficiency of three-coil LCT can be deduced as (12) and (13), as shown at the bottom of the next page.

III. PROPOSED THREE-COIL LCT WITH MOVEABLE INTERMEDIATE COIL

The higher misalignment tolerance of system efficiency of LCT means lower decline of the efficiency under misalignment condition. Consequently, enhancing the efficiency of LCT when the offset reaches the maximum value should

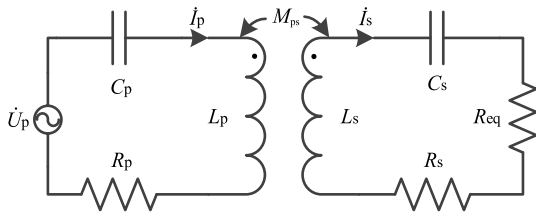


FIGURE 1. Equivalent circuit of two-coil LCT.

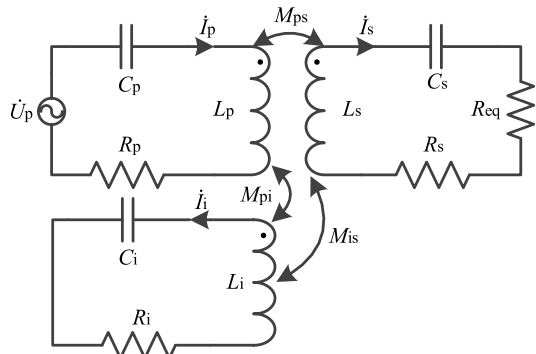
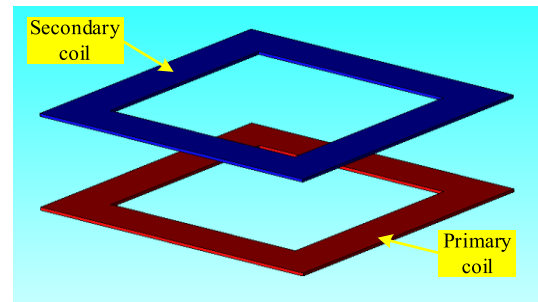
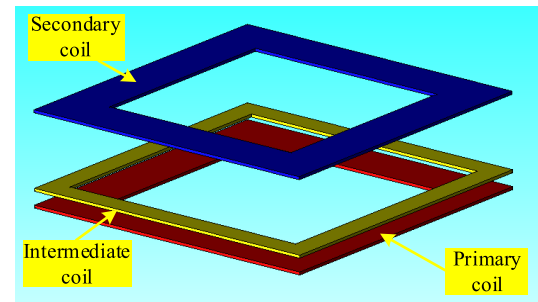


FIGURE 2. Equivalent circuit of three-coil LCT.



(a)



(b)

FIGURE 3. Finite element model. (a) Two-coil LCT. (b) Three-coil LCT.

be considered during the design of LCT. To study how to improve misalignment tolerance of efficiency by virtue of movable intermediate coil, the influence of compensation parameter and physical position of the intermediate coil on efficiency are studied in this section, and the results are compared with two-coil WPT.

This paper focuses on the influence of compensation parameter and physical position of the intermediate coil and proposing an adjustment strategy consequently. Therefore, the parameters of primary coil, secondary coil and intermediate coil are assumed to be known, and the corresponding optimization of coils is not described in this paper. To study the difference between three-coil LCT and two-coil LCT, and the influence of position and compensation parameter of intermediate coil on system efficiency, two-coil LCT and

three-coil LCT are modeled in finite element simulation software, as shown in Fig. 3(a) and (b). The outer diameter of the intermediate coil is set to be the same as that of the primary and secondary coil, and the detailed parameters are given in Table 1.

The adopted structure of three-coil LCT is shown in Fig. 3(b). The intermediate coil is placed slightly above the primary coil to facilitate its movement, and the intermediate coil can be removed to get a two-coil LCT as a contrast. The distance between primary and secondary coils is fixed at 200 mm, and the distance between primary and intermediate coils is fixed at 30 mm. The above structure is modeled in the finite element simulation software to calculate the performance of WPTs, and the parameters of three-coil LCT and two-coil LCT are listed in Table 1.

$$i_p = \frac{U_p (\omega^2 M_{is}^2 + Z_i Z_s)}{\omega^2 M_{is}^2 Z_p + \omega^2 M_{ps}^2 Z_i + \omega^2 M_{pi}^2 Z_s + Z_p Z_i Z_s - 2j\omega^3 M_{ps} M_{pi} M_{is}} \quad (9)$$

$$i_i = \frac{U_p (\omega^2 M_{ps} M_{is} + j\omega M_{pi} Z_s)}{\omega^2 M_{is}^2 Z_p + \omega^2 M_{ps}^2 Z_i + \omega^2 M_{pi}^2 Z_s + Z_p Z_i Z_s - 2j\omega^3 M_{ps} M_{pi} M_{is}} \quad (10)$$

$$i_s = \frac{U_p (\omega^2 M_{pi} M_{is} + j\omega M_{ps} Z_i)}{\omega^2 M_{is}^2 Z_p + \omega^2 M_{ps}^2 Z_i + \omega^2 M_{pi}^2 Z_s + Z_p Z_i Z_s - 2j\omega^3 M_{ps} M_{pi} M_{is}} \quad (11)$$

$$P_{out} = \frac{U_p^2 |\omega^2 M_{pi} M_{is} + j\omega M_{ps} Z_i|^2 R_{eq}}{|\omega^2 M_{is}^2 Z_p + \omega^2 M_{ps}^2 Z_i + \omega^2 M_{pi}^2 Z_s + Z_p Z_i Z_s - 2j\omega^3 M_{ps} M_{pi} M_{is}|^2} \quad (12)$$

$$\eta = \frac{|\omega^2 M_{pi} M_{is} + j\omega M_{ps} Z_i|^2 R_{eq}}{|\omega^2 M_{is}^2 + Z_i Z_s| |\omega^2 M_{is}^2 Z_p + \omega^2 M_{ps}^2 Z_i + \omega^2 M_{pi}^2 Z_s + Z_p Z_i Z_s - 2j\omega^3 M_{ps} M_{pi} M_{is}|} \quad (13)$$

TABLE 1. Parameters of cases.

Parameters	Two-coil	Three-coil
Primary voltage U_p (V)	255	255
Equivalent load resistance R_{eq} (Ω)	50	50
System operating frequency f_o (kHz)	85	85
Self-inductance of primary coil L_p (μ H)	321.83	321.83
Self-inductance of secondary coil L_s (μ H)	314.97	314.97
Self-inductance of intermediate coil L_i (μ H)	-	46.504
Resistance of primary coil R_p (Ω)	1	1
Resistance of secondary coil R_s (Ω)	1	1
Resistance of intermediate coil R_i (Ω)	-	0.5
Mutual-inductance between the primary and the secondary coil M_{ps} (μ H)	59.524	59.524
Mutual-inductance between primary and intermediate coil M_{pi} (μ H)	-	39.064
Mutual-inductance between intermediate and secondary coil M_{is} (μ H)	-	19.294
Size of primary and secondary coil (mm)	700×700×6.5	700×700×6.5
Size of intermediate coil (mm)	-	700×700×6.5

A. ANALYSIS OF INTERMEDIATE COIL'S COMPENSATION PARAMETER

For two-coil WPT system, S/S compensation is widely used for its simple structure and excellent performance. The maximum efficiency can be achieved when the compensation parameter satisfies the following formula, which means the circuit is under resonant condition.

$$\begin{cases} C_{pres} = \frac{1}{\omega^2 L_p} \\ C_{sres} = \frac{1}{\omega^2 L_s} \end{cases} \quad (14)$$

Substituting the parameters of two-coil LCT in Table 1, the efficiency can be calculated to be 95.42%. For more intuitive comparison, the primary and secondary compensation parameters of the three-coil LCT are set to be the same as that of two-coil LCT. Then, the influence of intermediate coil's compensation parameter on system efficiency is shown in Fig. 4. To compare with the resonant capacitance parameter, the independent variable is set as the ratio of the intermediate coil's compensation parameter to the resonant capacitance parameter. As can be concluded from Fig. 4, when the resonant capacitance parameter of intermediate is adopted the system efficiency isn't the highest point, and it's even lower than the efficiency of two-coil LCT.

The above discussion of intermediate coil's compensation parameter is on the premise that the receiving coil is aligned. Therefore, based on the above discussion, the intermediate coil's compensation is set to be C_{iopt} . Then, two-coil system, three-coil system with $C_i = C_{ires}$, and three-coil system with $C_i = C_{iopt}$ under misalignment condition are simulated. The simulated efficiency results are shown in Fig. 5. It is evident that the efficiency of three-coil system with $C_i = C_{iopt}$ is still higher than two-coil system and three-coil system with $C_i = C_{ires}$. In addition, when the receiving coil at the maximum offset 300mm, the efficiency decline of three-coil system with $C_i = C_{iopt}$ is also the smallest.

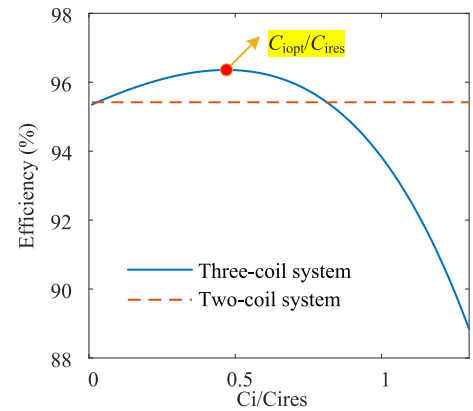


FIGURE 4. Influence of intermediate coil's compensation parameter on efficiency of three-coil LCT system compared with two-coil LCT system.

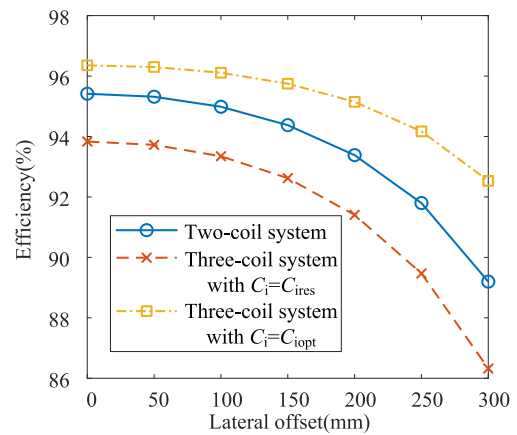


FIGURE 5. Efficiency under misalignment condition of three different systems.

B. ANALYSIS OF LCT SYSTEM WITH A MOVABLE INTERMEDIATE COIL

In a three-coil LCT system without magnetic core, the change of intermediate coil's position mainly affects the coupling coefficient between intermediate coil and primary or secondary coils. Firstly, the influence of coupling coefficient between intermediate coil and primary or secondary coils on system efficiency is studied. When the inductance parameters and mutual inductance between primary and secondary coil in Table 1 is adopted, the variation of the efficiency of three-coil LCT with k_{pi} and k_{is} is given in Fig. 6, where k_{ps} is the coupling coefficient between the primary and the secondary coil, k_{pi} is the coupling coefficient between the primary and the intermediate coil, and k_{is} is the coupling coefficient between the intermediate and secondary coil. To observe the influence of k_{pi} and k_{is} on system efficiency more intuitively, the top view of Fig. 6 is shown in Fig. 7. The darkest red area in Fig. 7 shows the collection of (k_{is}, k_{pi}) that can make the system efficiency reach the maximum with different k_{is} .

However, the collection of (k_{is}, k_{pi}) that can make the system efficiency reach the maximum value may not be obtained by adjusting the position of intermediate coil.

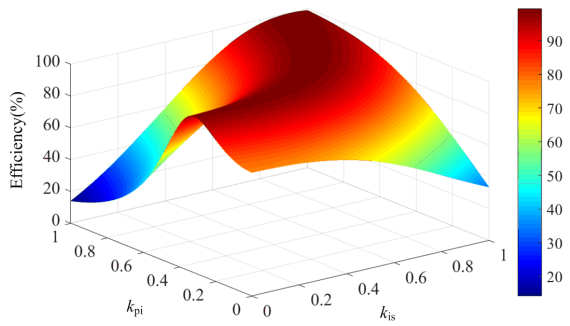


FIGURE 6. Variation of system efficiency with k_{pi} and k_{is} .

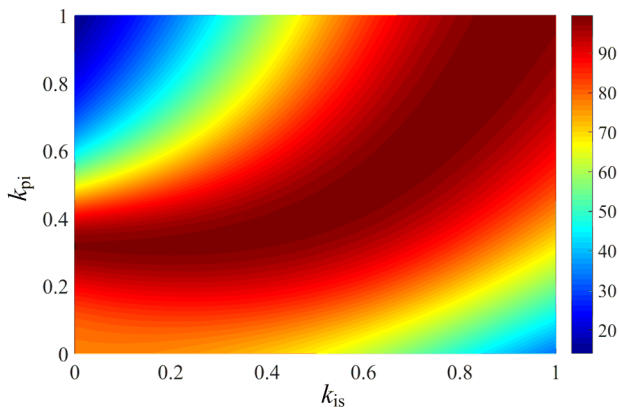


FIGURE 7. Top view of variation of system efficiency with k_{pi} and k_{is} .

Therefore, to simplify the analysis and make the conclusion more feasible, the influence of the position of intermediate coil on system efficiency under different misalignment of secondary coil will be studied next. It's worth noting that only the horizontal offset will be considered in this paper. Through finite element simulation, the efficiency of LCT system under different misalignment of secondary and intermediate coils can be obtained as shown in Fig. 8, where X_s and X_i represent offset of secondary and intermediate coils respectively. It can be concluded from Fig. 8 that there is an optimal position of intermediate coil to maximize system efficiency under different misalignment of secondary coil. In addition, the optimal position of intermediate coil $X_{i,opt}$ isn't the same as the position of secondary coil, but is slightly less than X_s .

Then, based on the data in Fig. 8, the optimal positions of intermediate coil at different X_s are sorted out, as shown in Fig. 9. It's evident that the relationship between $X_{i,opt}$ and X_s is $X_{i,opt} = X_s/2$. According to the position relationship of X_s and $X_{i,opt}$ in Fig. 9, the system efficiency of three-coil system with adjusted $X_i = X_{i,opt}$ is shown in Fig. 10. Compared with three-coil system with fixed $X_i = 0\text{mm}$, the decrease of system efficiency under misalignment condition is obviously reduced.

When the secondary coil is offset by 300mm, the distribution of flux density with fixed and optimal position of intermediate coil is shown in Fig. 11. By adjusting the position of the intermediate coil under the misalignment

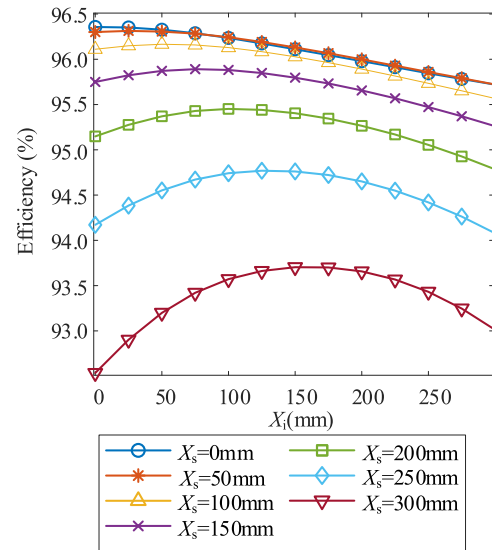


FIGURE 8. System efficiency under different misalignment of secondary and intermediate coils.

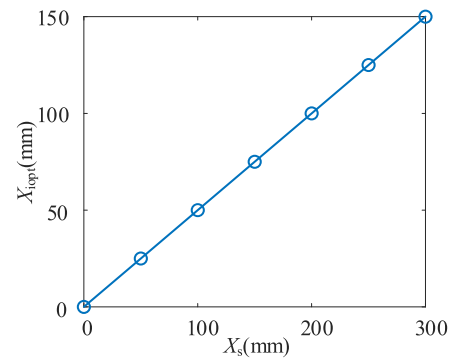


FIGURE 9. Optimal positions of intermediate coil at different position of secondary coil.

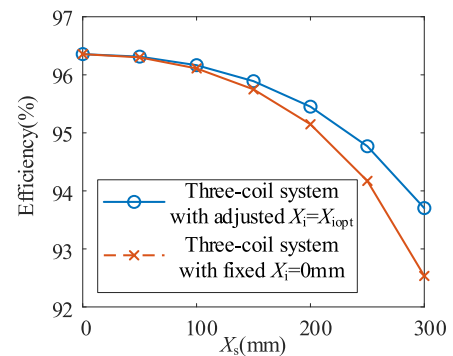


FIGURE 10. The efficiency comparison between three-coil system with adjusted $X_i = X_{i,opt}$ and three-coil system with fixed $X_i = 0\text{mm}$.

condition, the magnetic flux coupling between the transmitter and receiver is greatly enhanced, so the movable intermediate coil can enhance the misalignment tolerance.

C. ANALYSIS OF THE INFLUENCE OF ADJUSTABLE SYSTEM FREQUENCY

The compensation capacitance parameter of the intermediate coil is selected as the optimal value when the secondary coil

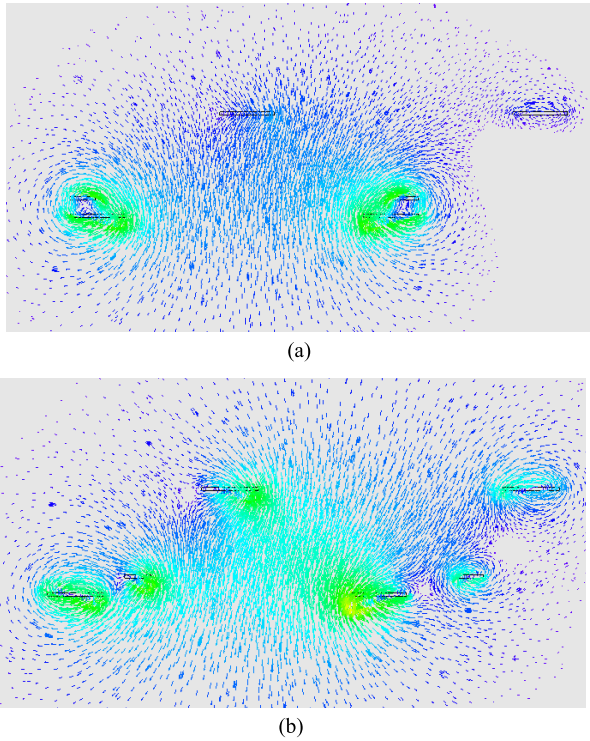


FIGURE 11. The distribution of flux density with fixed and optimal position of intermediate coil. (a) Fixed position of intermediate coil. (b) Optimal position of intermediate coil.

and the intermediate coil are both aligned. However, when the secondary coil is offset and the position the intermediate coil is adjusted accordingly, the optimal compensation parameter changes, and the compensation capacitance needs to be adjusted accordingly to maximize the efficiency. Considering the difficulty of adjusting capacitance parameter in the actual system, the adjustable system frequency is adopted in this paper.

According to the previous analysis, the optimal position of intermediate coil is 150mm, while the offset of secondary coil is 300mm. With the above cases, the effect of variable frequency on the system efficiency is analyzed, as shown in Fig. 12. It's evident that the highest efficiency is realized when the frequency deviates from the rated frequency. Therefore, the misalignment tolerance of efficiency can be further improved by adjusting system frequency to improve the efficiency when the secondary coil is not aligned.

D. CONTROL STRATEGY OF LCT SYSTEM WITH MOVABLE INTERMEDIATE COIL AND ADJUSTABLE FREQUENCY

According to the above analysis, when the secondary coil is not aligned, the position of intermediate coil and system frequency both affect the system efficiency. By adjusting the position of the intermediate coil and system frequency, the system efficiency under different misalignment condition can be maximized. The flowchart of detailed control strategy is shown in Fig. 13, including position adjustment control and frequency tracking control.

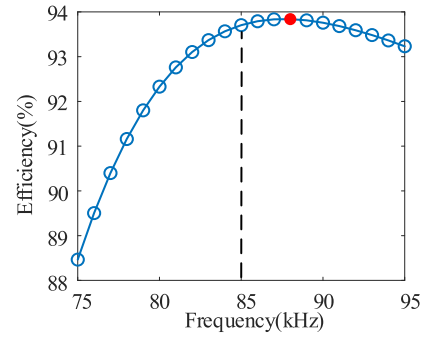


FIGURE 12. Effect of variable frequency on system efficiency.

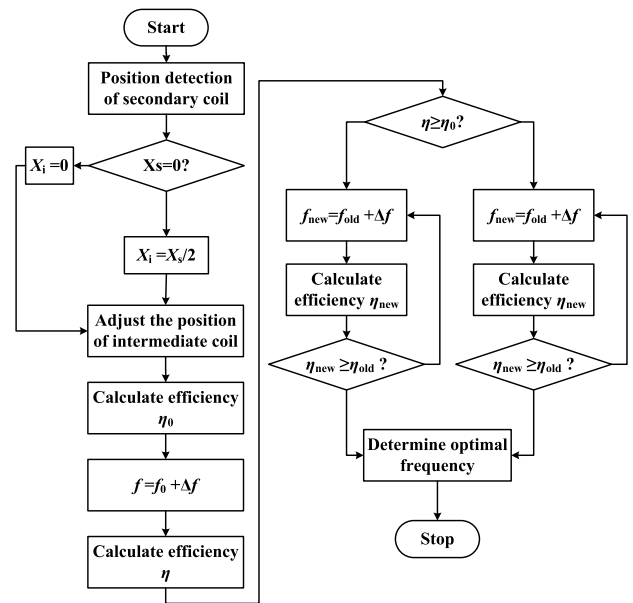


FIGURE 13. Flowchart of detailed control strategy.

Firstly, the position of secondary coil is detected and the initial frequency is set as 85-kHz. Then, the position of intermediate coil is adjusted to half of the offset position of the secondary coil, according to Section III.B. The frequency tracking procedure is performed subsequently to maximize the system efficiency.

Finally, characteristics of the proposed three-coil LCT are as follows. 1) The intermediate coil is slightly higher than primary coil; 2) The outer diameter of intermediate coil is same as the primary and secondary coils; 3) The system frequency is variable; 4) The intermediate coil can move according to the misalignment of secondary coil.

IV. EXPERIMENTAL VALIDATION

A. PROTOTYPE AND EXPERIMENTAL SETUP

To validate the feasibility of the proposed control strategy for the LCT with movable intermediate coil and adjusted frequency, a prototype of WPT system is manufactured and shown in Fig. 14. The parameters of the prototype are shown in Table 2. The test platform includes DC power supply,

TABLE 2. Parameters of prototype WPT.

Parameters	Value
Equivalent load resistance R_{eq} (Ω)	50
Rated operating frequency f (kHz)	85
Self-inductance of primary coil L_p (μ H)	309.3
Self-inductance of secondary coil L_s (μ H)	314.1
Self-inductance of intermediate coil L_i (μ H)	100.5
Primary resonant capacitance value C_{prs} (nF)	11.35
Secondary resonant capacitance value C_{strs} (nF)	11.18
Intermediate resonant capacitance value C_{irs} (nF)	34.92
Mutual inductance between primary and secondary coil M_{ps}	76.76
Mutual inductance between primary and intermediate coil M_{pi}	116.94
Mutual inductance between intermediate and secondary coil M_{is}	48.28
Resistance of primary coil R_p (Ω)	0.6
Resistance of secondary coil R_s (Ω)	0.5
Resistance of intermediate coil R_i (Ω)	0.3

high frequency inverter with adjustable switching frequency, a three-coil LCT, three compensating capacitor banks made by film capacitors, and non-inductive load resistor.

The LCT consist of three layers coils which wound by the Litz wire with a radius of 6.5 mm, the size of the primary and secondary coils is 700×700 mm, the size of the intermediate coil is also 700×700 mm. The distance between primary and secondary coils is fixed at 200mm, and the distance between primary and intermediate coils is fixed at 30mm, which is same as the air gap distance in simulation.

The physical parameters of the test rig are measured by the impedance analyzer and the circuit parameters of the test rig are measured by the precise power analyzer.

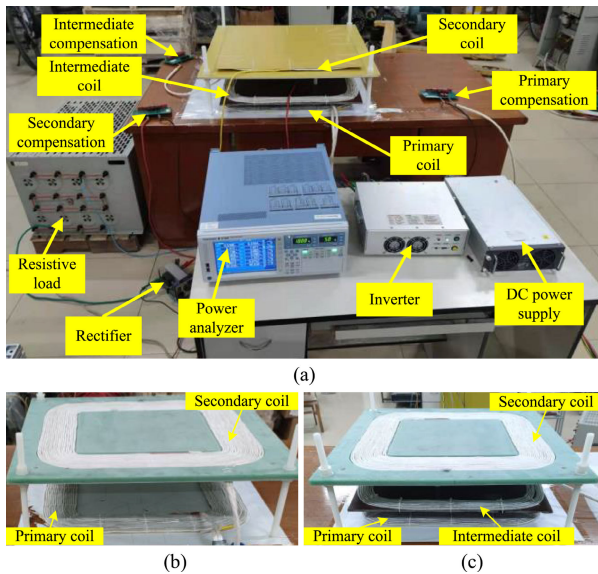


FIGURE 14. Experimental platform. (a) Test rig. (b) Two-coil LCT. (c) Three-coil LCT.

B. COMPARISON BETWEEN THE TWO-COIL AND THREE-COIL LCT

In the experimental verification, the advantage of three-coil LCT in improving the misalignment tolerance of efficiency

is compared with two-coil LCT. After selecting the compensation parameter of intermediate coil according to the method mentioned above, the efficiency of two-coil and three-coil LCT under the alignment condition are tested by using the high precise power analyzer, as shown in Fig.15. It can be seen that the efficiency of three-coil LCT is higher than two-coil LCT when the output power is both 3 kW. Then, the variations of the efficiency of two-coil and three-coil LCT with lateral offset are shown in Fig. 16. It can be concluded that.

1) With the increase of lateral offset, the efficiency of two-coil and three-coil LCT both decreases.

2) At different offset positions, the efficiency of the three-coil system is higher than that of the two-coil system. With the increase of lateral offset, the effect of intermediate coil in improving efficiency is increasing.



FIGURE 15. Measured results of two-coil and three-coil LCT under the alignment condition. (a) Two-coil LCT. (b) Three-coil LCT.

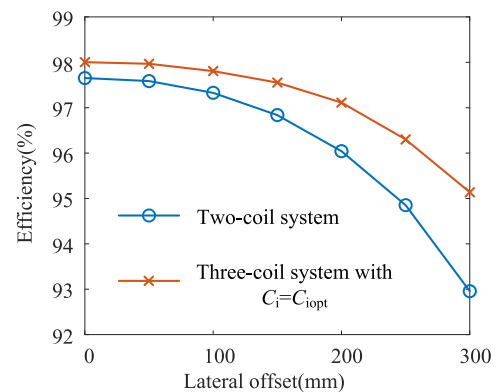


FIGURE 16. Variations of the efficiency of the two-coil and three-coil LCT with lateral offset.

C. COMPARISON BETWEEN THREE-COIL LCT WITH AND WITHOUT CONTROL STRATEGY

Based on the comparison of three-coil and two-coil LCT above, the control strategy of intermediate coil's position and system frequency proposed in this paper is verified. During the experiment, when the secondary coil is offset laterally, the position of intermediate coil and system frequency are adjusted. According to the simulation analysis above, the optimal position of intermediate coil is half of X_s , and the adjustment of position intermediate coil and system follows the process in Fig. 12. The lateral offsets of secondary coil are obtained directly from the scale on coils.

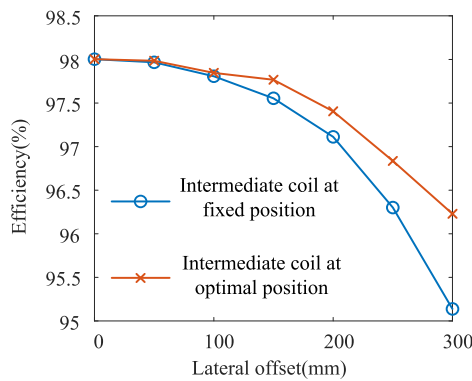


FIGURE 17. Variations of the efficiencies of the two-coil and three-coil LCTs with lateral offset.



FIGURE 18. Test result of three-coil LCT with movable intermediate coil at the maximum offset.

By using the high precise power analyzer, with movable intermediate coil at optimal position and adjusted system frequency, the efficiency of three-coil LCT under misalignment condition is measured and shown in Fig. 17, and the measured waveforms when lateral offset reaches 300mm are shown in Fig. 18. Channel 3 measures the input voltage/current of primary coil, and the channel 4 measures the output voltage/current of secondary coil. It's evident that the efficiency of three-coil LCT can be further improved under the misalignment condition. When the lateral offset of secondary coil reaches 300mm, the efficiency of three-coil LCT can be improve by 3.3% compared with two-coil LCT. It can be concluded that.

1) Comparing to the three-coil LCT with intermediate coil at fixed position, when the lateral offset is no more than 100mm, the effect of moveable intermediate coil in improving efficiency is not obvious.

2) When the lateral offset is more than 100mm, with the increase of lateral offset, the effect of moveable intermediate coil in improving efficiency is increasing.

V. CONCLUSION

To improve the misalignment tolerance of efficiency of WPT system, this study proposed a three-coil LCT with movable

intermediate coil and adjustable frequency. Main conclusions are as follows.

1) The influence of the intermediate coil's compensation parameter on the efficiency of three-coil LCT is studied and compared with the efficiency of two-coil LCT. Afterward, the efficiency of three-coil LCT with optimized intermediate coil's compensation parameter under misalignment condition is compared with the two-coil LCT.

2) Then, the influence of the position of the intermediate coil and system frequency on the efficiency of LCT with lateral offset was studied, and a control strategy of the intermediate coil's position and system frequency was proposed to promote the misalignment tolerance of efficiency.

3) A 3-kW prototype WPT with three-coil LCT was designed and manufactured, and the effectiveness of the proposed control strategy for system efficiency was also verified. Experimental results showed that the proposed strategy can effectively suppress the efficiency decline, improving the misalignment tolerance of WPT.

REFERENCES

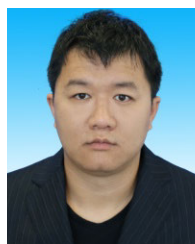
- [1] H. H. Eldeeb, A. T. Elsayed, C. R. Lashway, and O. Mohammed, "Hybrid energy storage sizing and power splitting optimization for plug-in electric vehicles," *IEEE Trans. Ind. Appl.*, vol. 55, no. 3, pp. 2252–2262, May/June 2019.
- [2] Y. Liu, U. K. Madawala, R. Mai, and Z. He, "Zero-phase-angle controlled bidirectional wireless EV charging systems for large coil misalignments," *IEEE Trans. Power Electron.*, vol. 35, no. 5, pp. 5343–5353, May 2020.
- [3] K. A. Cota, P. A. Gray, M. Pathmanathan, and P. W. Lehn, "An approach for selecting compensation capacitances in resonance-based EV wireless power transfer systems with switched capacitors," *IEEE Trans. Transport Electric.*, vol. 5, no. 4, pp. 1004–1014, Dec. 2019.
- [4] Z. Zhang, W. Ai, Z. Liang, and J. Wang, "Topology-reconfigurable capacitor matrix for encrypted dynamic wireless charging of electric vehicles," *IEEE Trans. Veh. Technol.*, vol. 67, no. 10, pp. 9284–9293, Oct. 2018.
- [5] D. H. Tran, V. B. Vu, and W. Choi, "Design of a high-efficiency wireless power transfer system with intermediate coils for the on-board chargers of electric vehicles," *IEEE Trans. Power Electron.*, vol. 33, no. 1, pp. 175–187, Jan. 2018.
- [6] S. Moon and G.-W. Moon, "Wireless power transfer system with an asymmetric four-coil resonator for electric vehicle battery chargers," *IEEE Trans. Power Electron.*, vol. 31, no. 10, pp. 6844–6854, Oct. 2016.
- [7] Q. Zhu, Y. Zhang, Y. Guo, C. Liao, L. Wang, and L. Wang, "Null-coupled electromagnetic field canceling coil for wireless power transfer system," *IEEE Trans. Transport Electric.*, vol. 3, no. 2, pp. 464–473, Jun. 2017.
- [8] Q. Zhu, Y. Zhang, C. Liao, Y. Guo, L. Wang, and F. Li, "Experimental study on asymmetric wireless power transfer system for electric vehicle considering ferrous chassis," *IEEE Trans. Transport Electric.*, vol. 3, no. 2, pp. 427–433, Jun. 2017.
- [9] M. Budhia, J. T. Boys, G. A. Covic, and C.-Y. Huang, "Development of a single-sided flux magnetic coupler for electric vehicle IPT charging systems," *IEEE Trans. Ind. Electron.*, vol. 60, no. 1, pp. 318–328, Jan. 2013.
- [10] A. Zaheer, G. A. Covic, and D. Kacprzak, "A bipolar pad in a 10-kHz 300-W distributed IPT system for AGV applications," *IEEE Trans. Ind. Electron.*, vol. 61, no. 7, pp. 3288–3301, Jul. 2014.
- [11] G. A. Covic, M. L. G. Kissin, D. Kacprzak, N. Clausen, and H. Hao, "A bipolar primary pad topology for EV stationary charging and highway power by inductive coupling," in *Proc. IEEE Energy Convers. Congr. Expo.*, Sep. 2011, pp. 1832–1838.
- [12] Z. Luo and X. Wei, "Analysis of square and circular planar spiral coils in wireless power transfer system for electric vehicles," *IEEE Trans. Ind. Electron.*, vol. 65, no. 1, pp. 331–341, Jan. 2018.
- [13] M. Budhia, G. Covic, and J. Boys, "A new IPT magnetic coupler for electric vehicle charging systems," in *Proc. 36th Annu. Conf. IEEE Ind. Electron. Soc. (IECON)*, Nov. 2010, pp. 2487–2492.

- [14] K. Ahmed, M. Aamir, M. K. Uddin, and S. Mekhilef, "A new coil design for enhancement in misalignment tolerance of wireless charging system," in *Proc. IEEE Student Conf. Res. Develop. (SCORED)*, Dec. 2015, pp. 215–219.
- [15] Q. Deng, J. Liu, D. Czarkowski, M. K. Kazimierczuk, M. Bojarski, H. Zhou, and W. Hu, "Frequency-dependent resistance of litz-wire square solenoid coils and quality factor optimization for wireless power transfer," *IEEE Trans. Ind. Electron.*, vol. 63, no. 5, pp. 2825–2837, May 2016.
- [16] Z. Wang, S. Cui, S. Han, K. Song, C. Zhu, M. I. Matveevich, and O. S. Yurievich, "A novel magnetic coupling mechanism for dynamic wireless charging system for electric vehicles," *IEEE Trans. Veh. Technol.*, vol. 67, no. 1, pp. 124–133, Jan. 2018.
- [17] M. Mohammad, S. Choi, Z. Islam, S. Kwak, and J. Baek, "Core design and optimization for better misalignment tolerance and higher range of wireless charging of PHEV," *IEEE Trans. Transport Electrific.*, vol. 3, no. 2, pp. 445–453, Jun. 2017.
- [18] C.-C. Hou, Y.-H. Teng, W.-P. Chang, and K.-Y. Chang, "Analysis and comparison of EE-type and CC-type cores for wireless power transfer systems," in *Proc. 9th Int. Conf. Power Electron. ECCE Asia (ICPE-ECCE Asia)*, Jun. 2015, pp. 1950–1954.
- [19] S. Moon, B.-C. Kim, S.-Y. Cho, C.-H. Ahn, and G.-W. Moon, "Analysis and design of a wireless power transfer system with an intermediate coil for high efficiency," *IEEE Trans. Ind. Electron.*, vol. 61, no. 11, pp. 5861–5870, Nov. 2014.
- [20] H. Zhao, Y. Wang, H. H. Eldeeb, Y. Zhan, G. Xu, and O. A. Mohammed, "Design of loosely coupled transformer for wireless power transfer for higher misalignment tolerance of system efficiency," in *Proc. IEEE Energy Convers. Congr. Expo. (ECCE)*, Baltimore, MD, USA, Sep. 2019, pp. 786–793.
- [21] Y. Wang, Y. Yao, X. Liu, D. Xu, and L. Cai, "An LC/S compensation topology and coil design technique for wireless power transfer," *IEEE Trans. Power Electron.*, vol. 33, no. 3, pp. 2007–2025, Mar. 2018.
- [22] E. G. Marques, C. Marques, J. V. N. S. V. da Silva, M. S. Perdigão, and A. M. S. Mendes, "Evaluation of intermediate coils in IPT systems under magnetic coupler displacements," in *Proc. 43rd Annu. Conf. IEEE Ind. Electron. Soc. (IECON)*, Nov. 2017, pp. 5342–5347.
- [23] W. Zhang and C. C. Mi, "Compensation topologies of high-power wireless power transfer systems," *IEEE Trans. Veh. Technol.*, vol. 65, no. 6, pp. 4768–4778, Jun. 2016.
- [24] W. Li, H. Zhao, J. Deng, S. Li, and C. C. Mi, "Comparison study on SS and double-sided LCC compensation topologies for EV/PHEV wireless chargers," *IEEE Trans. Veh. Technol.*, vol. 65, no. 6, pp. 4429–4439, Jun. 2016.
- [25] Q. Zhu, Y. Guo, L. Wang, C. Liao, and F. Li, "Improving the misalignment tolerance of wireless charging system by optimizing the compensate capacitor," *IEEE Trans. Ind. Electron.*, vol. 62, no. 8, pp. 4832–4836, Aug. 2015.
- [26] A. Kamineni, G. A. Covic, and J. T. Boys, "Analysis of coplanar intermediate coil structures in inductive power transfer systems," *IEEE Trans. Power Electron.*, vol. 30, no. 11, pp. 6141–6154, Nov. 2015.
- [27] Y. Chen, R. Mai, Y. Zhang, M. Li, and Z. He, "Improving misalignment tolerance for IPT system using a third-coil," *IEEE Trans. Power Electron.*, vol. 34, no. 4, pp. 3009–3013, Apr. 2019.



FUYAO YANG received the B.E. and M.E. degrees in materials science and engineering from the Harbin Institute of Technology (HIT), Harbin, China, in 2008 and 2010, respectively, and the Ph.D. degree in materials science from the University of Science and Technology Beijing (USTB), Beijing, China, in 2018.

He is currently a Research and Development Engineer with the State Key Laboratory of Advanced Power Transmission Technology, Global Energy Interconnection Research Institute Company, Ltd. His research interests include electromagnetic materials, electrical machines, and wireless power transfer.

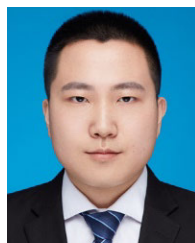


BO CAI received the B.E. degree in electrical engineering and automation from the Changsha University of Science and Technology, Changsha, China, in 2006, and the M.E. degree in electric machines and apparatus from North China Electric Power University (NCEPU), Beijing, China, in 2010.

He is currently a Research and Development Engineer with the State Key Laboratory of Advanced Power Transmission Technology, Global Energy Interconnection Research Institute Company, Ltd. His research interests include power electronics and drives, and wireless power transfer.



SONG LI received the B.E. degree in electrical engineering from North China Electric Power University, Baoding, China, in 2012, where he is currently pursuing the Ph.D. degree in electrical engineering. His research interests include wireless power transfer and electrical machines.



KUN LIU received the B.E. degree from North China Electric Power University, Beijing, China, in 2019, where he is currently a postgraduate student with the School of Electrical and Electronics Engineering.

His research interest includes wireless power transfer.



HAISEN ZHAO (Senior Member, IEEE) received the B.E. degree in agricultural electrification and automation from the Agricultural University of Hebei, Baoding, China, in 2004, and the M.E. and Ph.D. degrees in electric machines and apparatus from North China Electric Power University (NCEPU), Beijing, China, in 2007 and 2011, respectively.

He was a Visiting Scholar at the Energy Systems Research Laboratory, Department of Electrical and Computer Engineering, Florida International University (FIU), Miami, FL, USA, from December 2018 to December 2019. He is currently an Associate Professor with the School of Electrical and Electronic Engineering, North China Electric Power University. He is the author and coauthor of more than 100 articles in peer-reviewed journals and major international conferences. He has 20 patents awarded in the area of electric machine design, control, and energy-saving technologies. His research interests include electrical motors design, diagnosis, energy analysis, and energy-saving technologies of electric machines and drive systems, and wireless power transfer.



LIBO TIAN received the B.E. degree in agricultural electrification and automation from the Agricultural University of Hebei, Baoding, China, in 2004, and the M.E. degree in mode recognition and intelligent systems from the Beijing Institute of Technology, Beijing, China, in 2006.

She is currently a Lecturer with the School of Mechanical and Electrical Engineering, Shijiazhuang University. Her research interests include modeling of electrical machines and electrical intelligent control.